© 2024 Journal of Pharmacy & Pharmacognosy Research, 12 (5), 900-910, 2024
ISSN 0719-4250
https://jppres.com

DOI: https://doi.org/10.56499/jppres23.1717_12.5.900

Original Article

Piceatannol-rich extract from *Passiflora edulis* Sims seeds attenuates morphological differentiation through the reduction of MITF mRNA expression and F-actin polymerization in UVB-induced hyperpigmented B16F10 cells

[El extracto rico en piceatannol de las semillas de *Passiflora edulis* Sims atenúa la diferenciación morfológica mediante la reducción de la expresión de ARNm de MITF y la polimerización de F-actina en células B16F10 hiperpigmentadas inducidas por UVB]

Paween Kunsorn[1], Witchuda Payuhakrit[1,2], Nasapon Povichit[3], Prasit Suwannalert[1,2*]

[1]Department of Pathobiology, Faculty of Science, Mahidol University, Bangkok, Thailand.
[2]Pathobiology Information and Learning Center, Department of Pathobiology, Faculty of Science, Mahidol University, Bangkok, Thailand.
[3]Detox (Thailand) Co., Ltd., Chiangmai, Thailand.
*E-mail: prasit.suw@mahidol.ac.th

Abstract

Context: Ultraviolet B (UVB) light irradiation causes skin problems by increasing cellular oxidants, melanogenesis, and morphological changes of melanocytes. The use of active compounds derived from plants to mitigate these problems has been studied. Piceatannol (PCT), a phytochemical in the phenolic group contained in *Passiflora edulis* fruit seed (PFS), has gained interest for its anti-melanogenesis effects. However, the inhibitory effect on morphological differentiation related to melanin production of PFS extract is absent.

Aims: To investigate the effect of PFS extract on the inhibition of morphological differentiation associated with microphthalmia-associated transcription factor (MITF) mRNA expression and F-actin polymerization in UVB-induced hyperpigmented B16F10 cells.

Methods: Three fractions of PFS extract were analyzed for their total phenolics, PCT proportion, and antioxidant capacity. The fraction with the highest PCT proportion and antioxidant activity was investigated for its reductive effects on cellular oxidants, number of melanin-containing cells, melanin content, MITF mRNA expression, and tyrosinase activity in UVB-induced B16F10 cells. Morphological differentiation, as well as F-actin polymerization and arrangement, were analyzed.

Results: The PFS-F3 extract showed the highest antioxidant effect related to the proportion of PCT and phenolic contents. It attenuated cellular oxidants, the number of melanin-containing cells, melanin content, MITF mRNA expression, and tyrosinase activity. Differentiation, polymerization, and the arrangement of F-actin of most UVB-irradiated cells were repressed after treatment with the extract.

Conclusions: The PFS extract rich in PCT attenuated morphological differentiation by suppressing the functions of MITF mRNA and F-actin polymerization through the reduction of cellular oxidants, resulting in a decrease in melanin production.

Keywords: F-actin polymerization; hyperpigmentation; oxidative stress; passion fruit seed; piceatannol.

Resumen

Contexto: La irradiación con luz ultravioleta B (UVB) causa problemas cutáneos al aumentar los oxidantes celulares, la melanogénesis y los cambios morfológicos de los melanocitos. Se ha estudiado el uso de compuestos activos derivados de plantas para mitigar estos problemas. El piceatannol (PCT), un fitoquímico del grupo fenólico contenido en la semilla de la fruta de *Passiflora edulis* (PFS), ha cobrado interés por sus efectos antimelanogénicos. Sin embargo, el efecto inhibidor sobre la diferenciación morfológica relacionada con la producción de melanina del extracto de PFS está ausente.

Objetivos: Investigar el efecto del extracto de PFS en la inhibición de la diferenciación morfológica asociada a la expresión de ARNm del factor de transcripción asociado a la microftalmia (MITF) y la polimerización de F-actina en células B16F10 hiperpigmentadas inducidas por UVB.

Métodos: Se analizaron tres fracciones de extracto de SFP para determinar sus fenólicos totales, la proporción de PCT y su capacidad antioxidante. La fracción con la mayor proporción de PCT y actividad antioxidante se investigó por sus efectos reductores sobre los oxidantes celulares, el número de células con melanina, el contenido de melanina, la expresión de ARNm de MITF y la actividad tirosinasa en células B16F10 inducidas por UVB. Se analizó la diferenciación morfológica, así como la polimerización y disposición de la F-actina.

Resultados: El extracto PFS-F3 mostró el mayor efecto antioxidante relacionado con la proporción de PCT y el contenido fenólico. Atenuó los oxidantes celulares, el número de células con melanina, el contenido de melanina, la expresión de ARNm de MITF y la actividad tirosinasa. La diferenciación, la polimerización y la disposición de la F-actina de la mayoría de las células irradiadas con UVB se reprimieron tras el tratamiento con el extracto.

Conclusiones: El extracto de PFS rico en PCT atenuó la diferenciación morfológica mediante la supresión de las funciones del ARNm de MITF y la polimerización de F-actina a través de la reducción de los oxidantes celulares, resultando en la disminución de la producción de melanina.

Palabras Clave: estrés oxidativo; hiperpigmentación; piceatannol; polimerización de F-actina; semilla de maracuyá.

ARTICLE INFO
Received: June 17, 2023.
Accepted: February 25, 2024.
Available Online: April 19, 2024.

AUTHOR INFO
ORCID: 0000-0002-1202-5753 (PK)
0000-0003-4648-4912 (WP)
0000-0002-4622-7310 (PS)

Abbreviations: ABTS: 2,2'-azino-bis-3-ethylbenzothioline-6-sulfonic acid; CREB: cAMP response element binding protein; DCFH-DA: 2,7 dichlorohydrofluorescein diacetate; DCT: DOPA-chrome tautomerase; FRAP: Ferric reducing antioxidant power; KA: kojic acid; L-DOPA: levo-dihydroxyphenylalanine; MITF: microphthalmia-associated transcription factor; MTT: 3-(4,5-dimethylthiazol-2-yl)-2,5-diphenyl-tetrazolium bromide; PBS: buffer saline; PCT: piceatannol; PFS: *Passiflora edulis* fruit seeds; PFS-F1: refluxing the dried, powdered of PFS (10 g) in 60% ethanol (100 mL) for 1 h; PFS-F2: PFS ethanolic extract (200 mL) was passed through an SP825 column followed with centrifugation. The precipitate was separated and dried; PFS-F3: ethanolic/SP825 solution partitioned with ethyl acetate and then dried; PI: propidium iodide; ROS: reactive oxygen species; TRP1: tyrosine related protein 1; TYR: tyrosinase; UT: untreated cells; UVB: ultraviolet B light irradiation.

INTRODUCTION

UVB radiation causes the generation of reactive oxygen species (ROS) molecules within the skin. Excessive amounts of ROS disrupt the homeostasis of the cells. Melanin pigment is considered a potent antioxidant molecule, but the excess generation of melanin results in skin hyperpigmentation. Ultraviolet B (UVB) light irradiation-induced melanogenesis is initiated by the up-regulation of cAMP, which subsequently mediates the microphthalmia-associated transcription factor (MITF). The activation of MITF has a relatively strong effect on the transcription and translation of tyrosinase (TYR), tyrosine-related protein 1 (TRP1), and DOPA-chrome tautomerase (DCT). TYR, the critical enzyme for melanogenesis, converts levo-dihydroxyphenyl-alanine (L-DOPA) to L-dopachrome. Then, TRP1 and DCT further convert L-dopachrome to a melanin pigment (Kamiński et al., 2022; Wu et al., 2019).

The morphological differentiation of melanocytes is also affected by the functions of MITF (Nguyen and Fisher 2019). Carreira et al. (2006) revealed that moderate MITF activity promotes the polymerization of actin fibers, while high levels of MITF promote melanocyte differentiation, resulting in the increment of large-sized cells with densely packed melanin pigments and the formation of dendritic branches. The differentiation and dendrite development in melanocytes are related to the assembly of F-actin, whereby its polymerization acts as a cytoskeleton and provides strength for membrane protrusions (Katoh et al., 2011).

The majority of the current treatments for anti-hyperpigmentation mainly focus on tyrosinase inhibition (Zolghadri et al., 2023), while melanocytic differentiation also plays a crucial step in melanin synthesis (Knapp and Iden et al., 2020). however, treatment on inhibition of morphological differentiation related to the melanin production is absent. Therefore, exploring treatments targeting the inhibition of morphological differentiation associated with melanin production could offer a more comprehensive and effective treatment strategy in the realm of anti-hyperpigmentation therapies. To date, the study of phytochemicals for reducing hyperpigmentation is still of interest to scholars (Alam et al., 2018). It has been reported that the seeds of passion fruit (*Passiflora edulis* Sims, *Passifloraceae*) contain large amounts of piceatannol (PCT), which shows antioxidant and anti-melanogenesis effects (Matsui et al., 2010; Rossi et al., 2008). However, the properties of *P. edulis* fruit seeds (PFS) extract that contains PCT on cellular differentiation and the expression of the gene that plays a pivotal role in both melanogenesis and morphological changes in UVB-induced B16F10 cells are limited. Hence, this study aims to investigate the effect of PFS extract on the inhibition of morphological differentiation, which is associated with MITF mRNA expression and F-actin polymerization in UVB-induced hyperpigmented B16F10 cells.

MATERIAL AND METHODS

Preparation of piceatannol (PCT) from *P. edulis* fruit seeds (PFS)

Three fractions of PFS extracts were obtained from the project of Chalortham et al. (2019). The extraction was carried out by refluxing the dried, powdered PFS (10 g) in 60% ethanol (100 mL) for 1 h. The solution was filtrated and evaporated until crude extract was obtained and named PFS-F1. Another set of PFS ethanolic extract (200 mL) was passed through an SP825 column, followed by centrifugation. The precipitate was separated and dried to obtain PFS-F2. The supernatant of the ethanolic/SP825 solution was partitioned with ethyl acetate. The separated ethyl acetate part was then dried to obtain PFS-F3. The extracts were stored at -20°C until they were used.

Total phenolic contents

The total amount of phenolics in the PFS extracts was evaluated using a Folin-Denis assay. The extracts were dissolved with 60% ethanol and then diluted with deionized water to various concentrations. Twenty microliters of diluted extracts were mixed with Folin-Denis reagent (Sigma-Aldrich, St. Louis, MO, USA) and deionized water at volumes of 100 and 1580 µL, respectively. The mixture was incubated with 7.5% w/v sodium bicarbonate, 300 µL at room temperature and in a dark environment for 30 min, after which, then, measured the light absorbance was measured with a spectrophotometer (Labomed, Inc., Los Angeles, CA, USA) at a wavelength of 765 nm.

Gallic acid (Sigma-Aldrich, St. Louis, MO, USA) was used as a positive control (Lawag et al., 2023).

The fingerprint of PCT

The fingerprint of the PCT in the PFS extracts was investigated by using the HPLC system (Waters 2695 equipped with Waters 2487 Dual λ Absorbance Detector, Waters, Milford, MA, USA) with the results compared against the standard PCT concentration at 200 µg/mL. The standard PCT (purity >98%) was purchased from TCI, Tokyo, Japan. The dried powder of PFS extracts (125 mg) was dissolved in 1 mL of 60% HPLC grade ethanol, followed by filtration through a 0.2 µm PES filter. Deionized water (A) and HPLC grade acetonitrile (B) were used as the mobile phase at a ratio of (A):(B) = 90:10% in the initiation period. Separation was performed by isocratic elution at a ratio of (A):(B) at 75:25% at a temperature of 45°C. The flow rate was set to 0.8 mL/min with the injection volume at 5 µL. The HPLC C18 column (250 × 4.6 mm, i.d. 5 µm, ACE, Scottland) was employed as a stationary phase. The UV spectra were detected at 320 nm (Chalortham et al., 2019). The area under the curve of the PCT was calculated and proportioned against other total presented peaks.

Antioxidant capacity

ABTS assay

2,2'-azino-bis-3-ethylbenzothioline-6-sulfonic acid (ABTS) (Sigma-Aldrich, St. Louis, MO, USA) was employed for measuring the scavenging activity of the PFS extracts against the ABTS radical. ABTS solution was prepared according to Rodboon et al. (2020) with some modifications. Seven millimolars of ABTS were dissolved with 2.3 mM of potassium peroxydisulfate in a solution with a ratio of 2:3 v/v. This mixture was then incubated for 12 h in dark conditions and then dissolved with 95% ethanol to adjust the absorbance to be between 0.80 ± 0.05 when measured at a wavelength of 734 nm. Two hundred microliters of PFS extracts were mixed with 1.8 mL of ABTS solution and then incubated for 30 min. The mixture was measured for its absorbance by a spectrophotometer at 734 nm. Trolox (Sigma-Aldrich, St. Louis, MO, USA) solution was used as a standard to equate the antioxidant effect of the sample.

FRAP assay

A ferric-reducing antioxidant power (FRAP) assay was applied to measure the ferric-reducing capacity of the sample. The FRAP reagent (Sigma-Aldrich, St. Louis, MO, USA) was prepared by mixing 25 mL of 0.1 M of acetate buffer (pH 3.6) in 25 mL of 10 mM of 2,4,6-tripyridyl-s-triazine and 2.5 mL of ferric chloride hexahydrate (Sigma-Aldrich, St. Louis, MO, USA) solution. Twenty microliters of PFS extract were mixed with 180 µL of FRAP solution. The mixture was incubated in dark conditions at room temperature for 15 min, followed by measurement by a microplate reader (Molecular Devices, San Jose, CA, USA) at a wavelength of 595 nm. Iron (III) sulfate heptahydrate ($FeSO_4.7H_2O$) (Sigma-Aldrich, St. Louis, MO, USA) was used as the standard for ferric reducing capacity (FRC) (Hobanthad and Maneetong, 2019).

Cell culture

B16F10 mouse melanoma cells (ATCC, Manassas, VA, USA) were cultured in low glucose Dulbecco's Modified Eagle Medium (DMEM, Sigma-Aldrich, St. Louis, MO, USA) supplemented with 10% FBS (Capricorn Scientific, Ebsdorfergrund, Germany), 1% penicillin/streptomycin (Thermo Fisher Scientific, Waltham, MA, USA), and 3.7 mg/mL of sodium bicarbonate. In a humidified incubator, the cells were incubated in 5% CO_2 at 37°C.

Cell viability

The safe concentration level of PFS extract and kojic acid (KA) (Sigma-Aldrich, St. Louis, MO, USA), as well as the intensity of UVB radiation, were assessed with B16F10 cells by 3-(4,5-dimethylthiazol-2-yl)-2,5-diphenyltetrazolium bromide (MTT) assay. Briefly, the cells were seeded in 96 well plates at 1 × 10^4 cells/well density and then treated with 200 µL of various concentrations of PFS extract or KA for 24 h. Another set of cultured cells was exposed to multiple intensities of UVB radiation using a UVB lamp (Phillips, Amsterdam, Netherlands), followed by 24 h of complete media maintenance. After incubation, 0.5 mg/mL of MTT solution for 100 µL was added to the treated cells and incubated for another 2 h. The supernatant was removed, and then 100 µL of dimethyl sulfoxide was added and measured with a microplate reader at a wavelength of 570 nm. The percentage of living cells was determined as related to the untreated cells (UT) (Pintor et al., 2020).

Flow cytometric analysis

The flow cytometric analysis was conducted to verify that the dosage of PFS extract and KA and the UVB radiation intensity did not adversely affect cell survival. The method employed was adapted from Rieger et al. (2011) with some modifications. In brief, B16F10 cells (5 × 10^6 cells/well) were initially seeded in 6-well plates and incubated for 24 h. Subsequently, the cells were treated with 2 mL of various PFS extract or KA concentrations for an additional 24 h. Another set of cultured cells was exposed to multiple

intensities of UVB radiation, followed by 24 h of complete media maintenance. After incubation, the cells were harvested through trypsinization, washed with buffer saline (PBS), resuspended in binding buffer, and stained with annexin V for 15 min in the dark refrigerator. Subsequently, the cells were washed with PBS and resuspended in 1% paraformaldehyde/PBS, followed by the addition of propidium iodide (PI) at a concentration of 1 µg/mL. The stained cells were then incubated in the dark for 15 min. Following staining, the viability of the cells was assessed using a flow cytometer (FACScan, Becton Dickinson, USA) for the subsequent analysis of the cell population.

Measurement of cellular oxidants

The cellular oxidants in the UVB-induced B16F10 cells were investigated by 2,7 dichlorohydrofluorescein diacetate (DCFH-DA) assay. Briefly, B16F10 cells (1×10^4 cells/well) were seeded in black 96 well plates followed by 24 h of incubation. The culture media were removed and then washed once with phosphate PBS, after which the cells were exposed to UVB radiation at 100 mJ/cm^2, followed by the addition of 200 µL of PFS extract or KA, then incubation for 24 h. The supernatant was removed, and the PBS was used for washing, followed by the addition of 200 µL of 10 µM DCFH-DA (Sigma-Aldrich, St. Louis, MO, USA) solution and incubation for 1 h. The cells were measured by a fluorescent microplate reader (TECAN, Männedorf, Switzerland) at 485/535 nm for excitation/emission, respectively. The results of the cellular oxidants were presented as percentages compared to those of UT, with 1 mM of KA used as a positive control (Rodboon et al., 2020).

Measurement of melanin content

To measure melanin content, the B16F10 cells (2.5×10^5 cells/well) were plated in 6 well plates and incubated for 24 h. Then, the cells were irradiated with UVB radiation (100 mJ/cm^2) followed by treatment of PFS extract or KA for 48 h (with daily treatment). After that, the cells were observed under an inverted microscope and the images were recorded in different magnifications for further analysis of the melanin-containing cells and morphological differentiation. After that, the cells were lysed by adding 200 µM of 1% Triton X-100 in 1 N sodium hydroxide and they were then shaken at 60 rpm at 80°C. Then, the solutions were centrifuged, and the supernatant was transferred to 96 well plates for measurement at OD 405 nm. The results of the melanin content and the determination of melanin-containing cells were presented as percentages compared to those of UT, with 1 mM of KA used as a positive control (Kim et al., 2023).

Measurement of MITF mRNA expression

B16F10 cells were seeded in 6 well plates (1×10^6 cells/well) and incubated for 24 h. The cells were exposed to 100 mJ/cm^2 of UVB radiation and then treated with PFS extract or KA. After 24 h of treatment, the total RNA was extracted using RNeasy kits (Qiagen, Germantown, MD, USA). The quality of the extracted RNA was determined using NanoDrop™ (Thermo Fisher Scientific, Waltham, MA, USA) at the ratio of absorbance of 260 and 280 nm. All samples were normalized to the same concentration of total RNA and then were employed for reverse transcription using ReverstraAce RT-PCR conversion kit (Toyobo, Tokyo, Japan) in accordance with the manufacturer's protocol. The real-time PCR was performed with an i-Taq SYBR Green RT-PCR master mix (Bio-Rad, Hercules, CA, USA) equipped with a real-time PCR machine (Thermo Fisher Scientific, Waltham, MA, USA). MITF served as the target gene and GAPDH served as an internal control. Primers were used, as shown in Table 1.

PCR parameters were set as 95°C for 30 s for denaturation, 40 cycles of denaturation at 95°C for 30 s, annealing at 55°C for 30 s and extension at 72°C for 20 s. The quantity of mRNA was calculated by the $2^{-\Delta\Delta Ct}$ values compared to the internal control of GAPDH for each reaction. KA (1 mM) was used as a positive control (Wu et al., 2018).

Measurement of tyrosinase activity

The cellular tyrosinase activity was investigated. B16F10 cells were seeded in 6 well plates (5×10^5 cells/well) and then incubated for 24 h. The cells were exposed to 100 mJ/cm^2 of UVB followed by PFS extract or KA treatment. After 24 h of treatment, the cells were washed with iced cold PBS and then lysed with PBS, 0.1% triton X-100 and 0.1 mM phenylmethanesulfonyl fluoride before being centrifuged to obtain the supernatant. The concentration of the total proteins in each reaction was normalized then, the supernatant (80 µL) reacted with 20 mM of L-DOPA (80 µL) (Sigma-Aldrich, St. Louis, MO, USA). The mixtures were agitated before the measurement of absorbance at 492 nm. The tyrosinase activity results were presented as percentages compared to those of the UT, with 1 mM of KA used as a positive control (Rodboon et al., 2020).

Table 1. Primers used for amplification of the genes.

Gene	F/W sequence (5'-3')	R/W sequence (5'-3')
MITF	AGAAGCTGGAGCATGCGAACC	GTTCCTGGCTGCAGTTCTCAAGAAC
GAPDH	AAGGTCATCCCAGAGCTGAA	CTGCTTCACCTTGA

Table 2. The score and criteria for differentiating morphology of melanocytes.

Score	Criteria
1+	Cell size 1-50 µm, bipolar spindle dendrites, fewer melanin pigments, and distribution lower than 50% of cytoplasm area
2+	Cell size 1-50 µm, bipolar spindle dendrites, fewer melanin pigments, and distribution higher than 50% of cytoplasm area
3+	Cell size larger than 51 µm, multipolar spindle without tip branches, some melanin pigments distribute throughout the cytoplasm area
4+	Cell size larger than 51 µm, multipolar spindle with tip branches, densely packed melanin pigments distribute throughout the cytoplasm area

Determination of morphological differentiation in melanin-containing cells

The differentiation of the B16F10 cells' morphology was observed after UVB radiation, followed by 48 h of PFS extract or KA daily treatments. The morphological appearances of the melanin-containing cells were observed and described at 400× magnification. One hundred melanin-containing cells were differentiated using the criteria defined by Rodboon et al. (2020), as shown in Table 2.

The differentiated cells of the PFS treatments were compared to the UT, with 1 mM of KA used as a positive control.

Analysis of F-actin polymerization and arrangement

The polymerization and arrangement of F-actin in the UVB-induced B16F10 cells were observed using an immunofluorescent staining technique. B16F10 cells were cultured on a coverslip at 2 × 10^3 cells/piece density. After 24 h of incubation, the cells were exposed to UVB radiation (100 mJ/cm^2), followed by the treatment of each PFS extract or KA for 24 h. The cells were washed and fixed by cold absolute methanol. The fixed cells were permeabilized with 0.25% Triton X-100 and then blocked with 1% bovine serum albumin. The cells were stained with a primary polyclonal antibody (anti-F-actin, ab130935, Abcam, Waltham, MA, USA) for 90 min, followed by the addition of a secondary antibody (Alexa Fluro® 488, Abcam, Waltham, MA, USA) for 30 min. Hoechst-33342 (Sigma-Aldrich, St. Louis, MO, USA) was added to stain the nucleus for 30 min. The cells were then observed under a fluorescent microscope (Olympus BX53, Tokyo, Japan), and the images were recorded (González-Gutiérrez et al., 2020).

Statistical analysis

All experiments were performed in triplicate in 3 different batches. The results are presented in mean ± SD. Analyses were performed with one-way ANOVA using PASW Statistics 18 software (IBM Corp., Armonk, NY, USA). Values of $p \leq 0.05$ were considered significant.

RESULTS

PFS extracts contain PCT-exerted antioxidant capacity

Three fractions of PFS extracts were evaluated for total phenolic content since the PCT is a member of the phenolics group. All fractions showed different amounts of phenolic content, with PFS-F1 showing the least phenolic content while PFS-F3 showed the significantly highest content (Table 3). Using HPLC analysis, fingerprints of the PCT in all fractions were detected at around 16 min, which was at the same retention time as the standard, and PFS-F3 contained the highest proportion of PCT against the total presented compounds (Fig. 1 and Table 3). Antioxidant effects were assessed by ABTS and FRAP assays to investigate their scavenging and ferric-reducing capacities, respectively. As with the trend of antioxidant capacities, PFS-F3 exhibited the most potent effects (Table 3). These results indicate that PFS-F3 has the most powerful antioxidant activity related to the amount of PCT. Hence, PFS-F3 merits further investigation of its anti-melanogenesis effects in UVB-induced B16F10 cells.

Table 3. Proportion of piceatannol (PCT), total phenolic contents, and total antioxidant activity in each PFS extract.

Assay	PFS-F1	PFS-F2	PFS-F3
Proportion of PCT (% of total presented peaks)	45.20 ± 3.81	65.31 ± 2.16 [a*]	70.16 ± 3.15 [a**, b*]
Total phenolics (g Gallic acid/ g sample)	0.184 ± 0.018	0.354 ± 0.011 [a*]	0.559 ± 0.02 [a**, b*]
Total antioxidant activity	0.064 ± 0.002	0.071 ± 0.003	0.105 ± 0.004 [a*, b*]
ABTS (mg Trolox equivalent/g sample)			
FRAP ($M\ FeSO_4.7H_2O$ equivalent/g sample)	0.007 ± 0.001	0.009 ± 0.002	0.014 ± 0.001 [a*, b*]

Results represent mean ± SD (n = 3). * and ** Statistical significance at p≤0.05, and p≤0.01, respectively. [a] compared to PFS-F1 and [b] compared to PFS-F2.

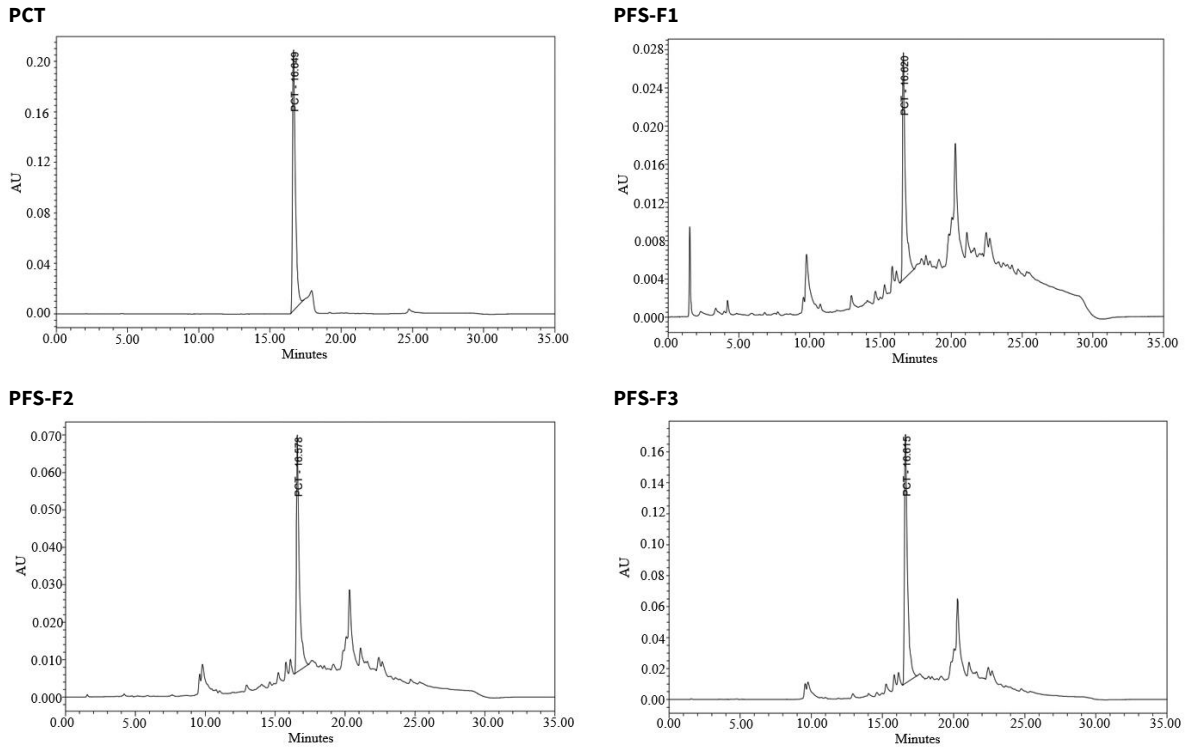

Figure 1. HPLC fingerprints of piceatannol (PCT) contained in each fraction of *P. edulis* fruit seed (PFS) extract.
The peak of PCT in all PFS extracts was detected at 16.6 min, comparable to that of the standard PCT, which also showed at 16.6 min.

PFS-F3 extract reduced cellular oxidants in UVB-induced B16F10

PFS-F3 extract and KA were evaluated to determine their safe concentrations with B16F10 cells by MTT assay and flow cytometric analysis for 24 h. Concentrations of 50 and 100 µg/mL of PFS-F3 extract and 1 mM of KA did not affect cell viability (Fig. 2A-B). The intensity of UVB radiation was also evaluated, and it was found that a 100 mJ/cm² intensity of UVB radiation did not cause cell death (Fig. 2A-B). Anti-cellular oxidants were investigated by DCFH-DA assay. B16F10 cells were cultured, exposed to UVB radiation, and then treated with the PFS-F3 for 24 h. It was found that UVB radiation increased cellular oxidants to a higher level than the UT. Treatment with the PFS-F3 extract lowered the level of cellular oxidants in a dose-dependent manner. PFS-F3 extract concentration of 100 µg/mL significantly reduced the cellular oxidants to a level lower than that of the UVB radiated cells (p≤0.05) (Fig. 2C). KA (1 mM), used as a positive control, reduced cellular oxidant levels to near those of PFS-F3 at 100 µg/mL. The results suggested that PFS-F3 extract can decrease cellular oxidants.

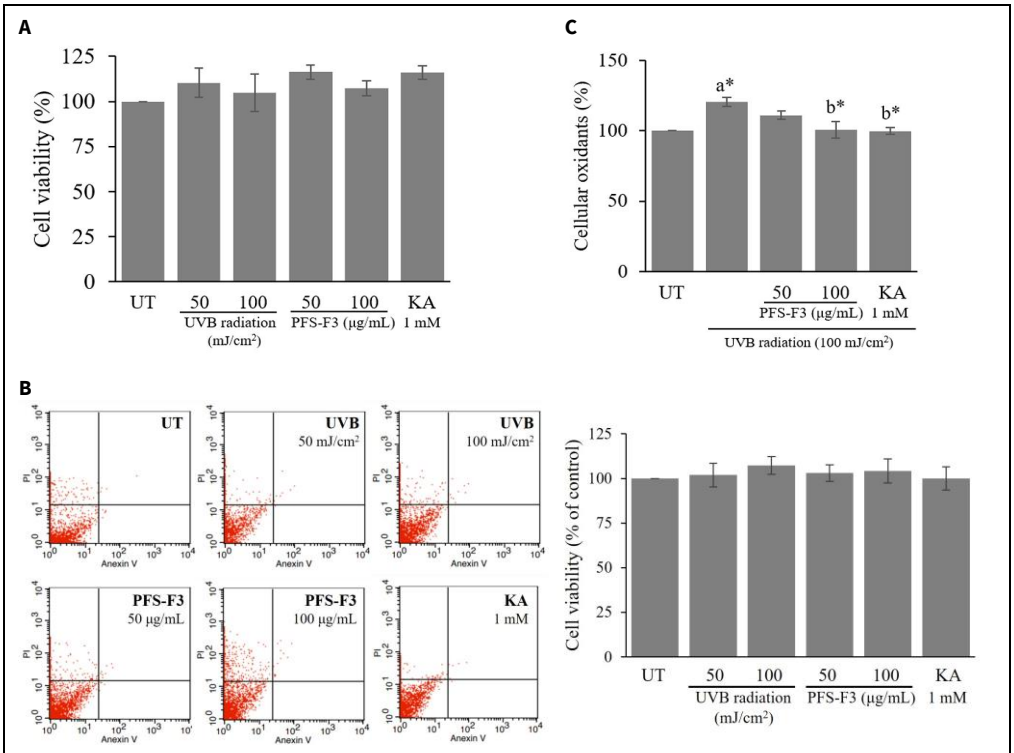

Fig. 2. Effect of PFS-F3 extract on the reduction of UVB-induced cellular oxidants.

(A) Safe intensities of UVB radiation, concentrations of PFS-F3, and kojic acid (KA) were investigated using the MTT assay. **(B)** Safe intensities of UVB radiation and concentrations of PFS-F3 and KA were investigated by flow cytometric analysis. **(C)** Cellular oxidants reductive effects of PFS-F3 extract. KA (1 mM) was used as a positive control. The data in graphs A, B, and C columns represent mean ± SD (n = 3). *Statistical significance at $p \leq 0.05$. [a]Compared to untreated cells (UT), [b]compared to UVB radiated cells.

PFS-F3 extract reduced UVB-induced melanogenesis

After UVB exposure followed by PFS-F3 treatments, B16F10 cells were observed, counted, and analyzed for the ratio of melanin-containing cells. UVB radiation significantly elevated the number of melanin-containing cells compared to the UT. Treatment of the extract lowered the number of melanin-containing cells in a dose-dependent manner with the maximal reduction at 100 μg/mL (Fig. 3A-B). Then, the cells were harvested to measure their melanin content. In accordance with the ratio of melanin-containing cells, UVB radiation elevated the number of melanin pigments. At the same time, PFS-F3 significantly suppressed the melanin content in a similar trend to that observed for the ratio of melanin-containing cells (Fig. 3C). KA (1 mM), used as a positive control, also significantly reduced melanin content compared to that of the UVB irradiated cells ($p \leq 0.01$). The results indicate that PFS-F3 extract can lower UVB-induced melanin production.

PFS-F3 extract suppressed MITF mRNA expression and its effect on the reduction of tyrosinase activity

The action of PFS-F3 extract on MITF mRNA expression was revealed by which the UVB radiation significantly elevated the expression of MITF mRNA compared to that of the UT. The treatment of PFS-F3 decreased MITF expression in a dose-dependent manner, with the most significant reduction being from 100 μg/mL compared to that of the UVB irradiated cells ($p \leq 0.05$) (Fig. 4A). Tyrosinase, a rate-limit substrate for melanogenesis, which MITF upregulates it, was also investigated. As expected, UVB radiation significantly increased the activity compared to the UT's. However, it was significantly lowered by the treatment of PFS-F3 (100 μg/mL, $p \leq 0.01$) (Fig. 4B). Kojic acid (KA, 1 mM), used as a positive control, also reduced the activity to near those of PFS-F3 at 100 μg/mL. This finding suggests that PFS-F3 extract has a capacity for the suppression of MITF mRNA expression, with tyrosinase activity decreasing as a consequence.

PFS-F3 extract reduced morphological changes by suppressing the dendritic formation associated with the polymerization and arrangement of F-actin

The morphology of the differentiated B16F10 cells was analyzed from a total of 100 melanin-containing cells, which were categorized into four groups according to their appearances as 1+, 2+, 3+, and 4+ (Fig. 5A). UVB radiation-induced the B16F10 cells to differentiate into score 3+ and 4+ by which the cells formed multiple dendrites. The number of differentiated cells with a score of 4+ was significantly higher than in the

UT (p≤0.05). However, treatment with PFS-F3 extract lowered the numbers of cells with scores of 3+ and 4+. In contrast, the populations of cells with scores of 1+ and 2+ were higher compared to those of the UVB irradiated cells (Fig. 5B). Associated with the dendritic formation, the polymerization and arrangement of F-actin were observed using immunofluorescent staining of the F-actin. The UT showed F-actin mildly clustered at the nucleus with a cellular margin, as seen in bright green. The UVB-irradiated cells exhibited polymerization of the F-actin fibers in numerous lines bundled in the cytoplasm, which was more potent than the UT. Moreover, the fibers were densely assembled, arranged across the nucleus, and localized at the cell branches. This indicates that the formation of dendrites is associated with the polymerization and organization of F-actin fibers. Treatment with the PFS-F3 extract lowered the formation and arrangement of F-actin fibers. Interestingly, PFS-F3 treatment at 100 µg/mL significantly decreased the polymerization of F-actin compared to the UVB irradiated cells, and the arrangement was at the cell border. Kojic acid (KA, 1 mM) treatment was used as a positive control and reduced the formation of dendrites and F-actin polymerization compared to that of the UVB irradiated cells (Fig. 5C). These results indicate that PFS-F3 extract lowered the differentiation of melanocytes by suppressing the formation of dendrites which are associated with the polymerization and arrangement of F-actin fibers.

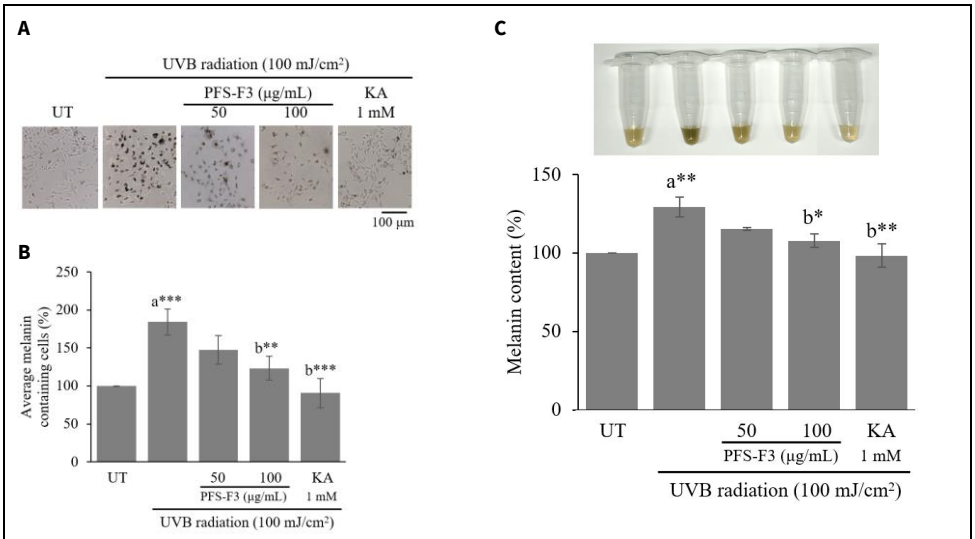

Fig. 3. Effects of PFS-F3 extract on the reduction of the ratio of melanin-containing cells and melanin content in UVB-induced B16F10 cells.

(A) Melanin-containing cells. **(B)** Ratio of melanin-containing cells calculated from the number of pigmented cells against all cells in the same visual field from a total of 1,000 cells. **(C)** Melanin content obtained from the extraction of the cells. Kojic acid (KA, 1 mM) was a positive control. Graph B and C data represent mean ± SD (n=3). *, **, *** Statistical significance was at p≤0.05, p≤0.01, and p≤0.001, respectively. [a]Compared to untreated cells (UT), [b]compared to UVB radiated cells.

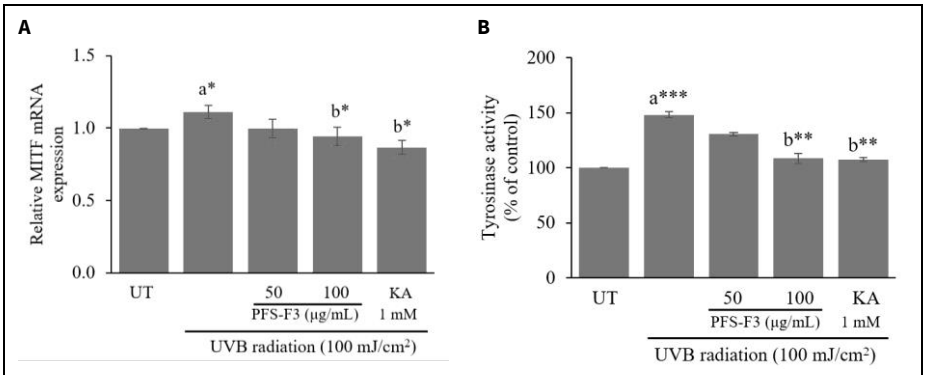

Fig. 4. Effects of PFS-F3 extract on the suppression of microphthalmia-associated transcription factor (MITF) mRNA expression and tyrosinase activity.

(A) MITF mRNA expression suppressive effect. The expression was performed by real-time PCR, and the values of the target genes were normalized to GAPDH before calculating the -ΔΔCt value. **(B)** Tyrosinase activity is derived from the reaction of cell lysates and L-DOPA. Kojic acid (KA, 1 mM) was a positive control. The graph is expressed in mean±SD and is relative to the untreated cells (UT) (n=3). *, **, *** Statistical significance at p≤0.05, p≤0.01, and p≤0.001, respectively. [a]Compared to the UT, [b]compared to UVB radiated cells.

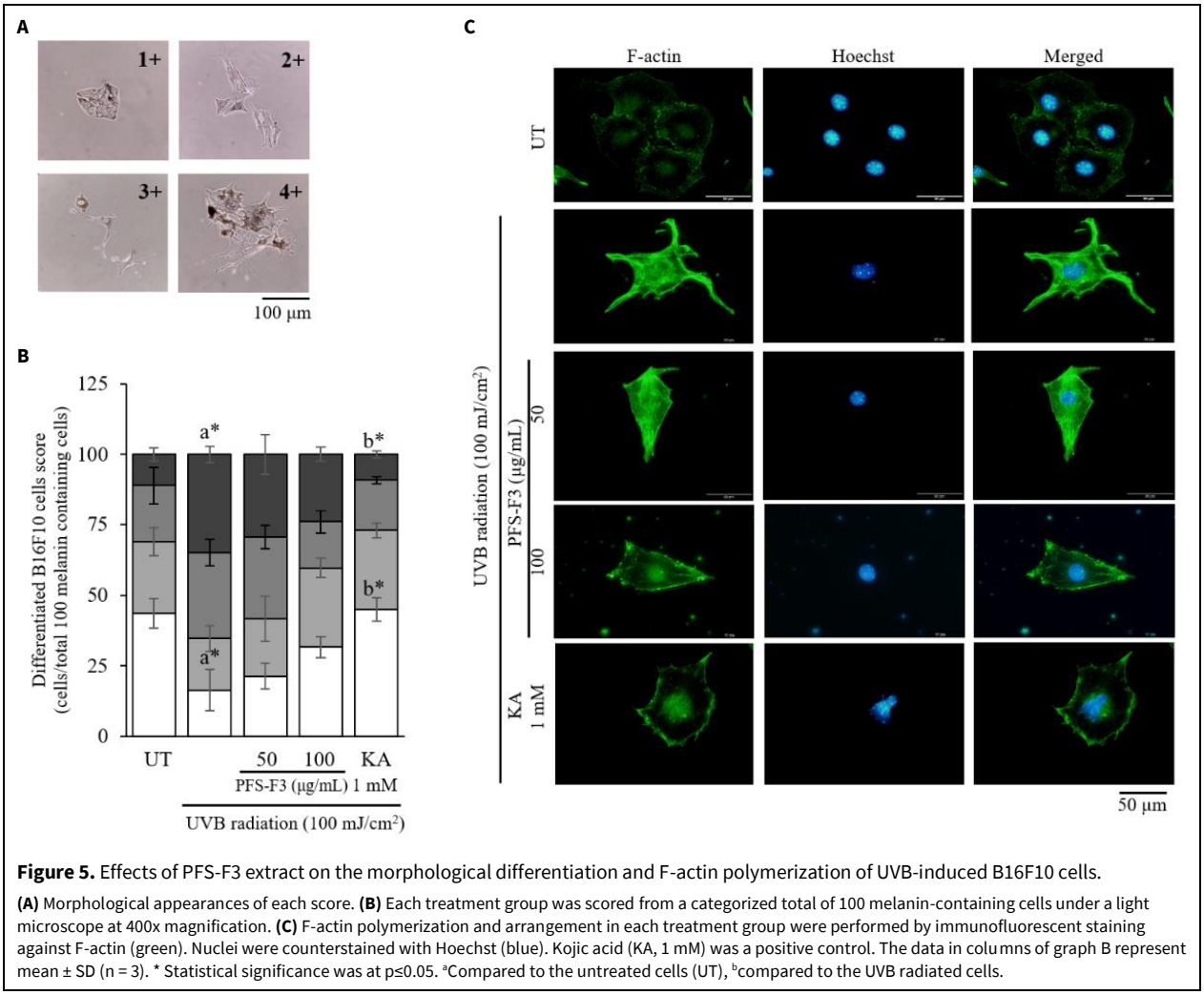

Figure 5. Effects of PFS-F3 extract on the morphological differentiation and F-actin polymerization of UVB-induced B16F10 cells.

(A) Morphological appearances of each score. **(B)** Each treatment group was scored from a categorized total of 100 melanin-containing cells under a light microscope at 400x magnification. **(C)** F-actin polymerization and arrangement in each treatment group were performed by immunofluorescent staining against F-actin (green). Nuclei were counterstained with Hoechst (blue). Kojic acid (KA, 1 mM) was a positive control. The data in columns of graph B represent mean ± SD (n = 3). * Statistical significance was at p≤0.05. [a]Compared to the untreated cells (UT), [b]compared to the UVB radiated cells.

DISCUSSION

PCT is a phenolic compound formed from the hydroxylation of resveratrol, which can be found in PFS. PCT exerts several properties, e.g., antioxidant, anticancer, and anti-inflammation, among others. (Matsui et al., 2010). In this study, as revealed by HPLC analysis, our results show that all fractions presented a PCT peak at a retention time of 16 min. Although PCT can also be detected in PFS-F1 and PFS-F2, it was found that PFS-F3 showed the highest proportion of PCT (compared to total presented compounds) related to phenolic contents. This reflects how separation and elution were able to sort out other compounds; thus, the amount of PCT was enhanced. The antioxidant effects revealed that PFS-F3 showed the most substantial reduction of oxidants by both scavenging free radical molecules and reducing free metal ions.

UVB radiation causes excessive oxidant molecules within the cells due to the high energy photons in the radiation directly hitting intracellular macro and micro molecules (Ravanat et al., 2001). As investigated by the DCFH-DA assay, PFS-F3 reduced UVB-induced cellular oxidants to a level below that of the irradiated cells. Upon UVB exposure, melanocytes are stimulated to produce transcription factors and initiate signaling pathways related to melanogenesis and morphological differentiation (Diaz-Camino et al., 2005). The important transcription factor for melanogenesis and differentiation is MITF. MITF is a critical factor in regulating the synthesis of melanogenesis and cellular differentiation-related enzymes: TYR, TRP1, and DCT (D'Mello et al., 2016). TYR, the critical enzyme for melanogenesis, converts L-DOPA to L-dopachrome. Then, TRP1 and DCT further convert L-dopachrome to melanin pigment and then transfer it out of the cell via the tips of the formed dendritic branches (D'Orazio et al., 2013). The differentiation and dendritic formation, including filopodia and lamellipodia in the melanocytes, are related to the polymerization of a cytoskeletal protein called F-actin (Li et al., 2020). Ishimoto and Mori (2022) reported that increased ROS induced by UVB irradiation enhanced F-actin polymerization. As our results

showed, UVB radiation-induced melanocytes to differentiate in large-sized cells with numerous dendrites and a dense accumulation of melanin pigment (grade 4+). PFS-F3 attenuates melanin production and maintains the melanocytes in grades 1+ and 2+, with these cells characterized as having a small, bipolar shape with less pigment. The decrement of tyrosinase activity inhibited melanogenesis due to the suppression of MITF mRNA expression. Cellular oxidants are reported to regulate the activity of MITF through the cAMP-CREB signaling pathway (Kawakami and Fisher, 2017). In this study, we propose that PCT lowered MITF expression due to its antioxidant capacity. The polymerization and arrangement of F-actin also decreased. Treatment with PFS-F3 extract at a concentration of 100 µg/mL markedly inhibited F-actin's polymerization and arrangement. Therefore, the lower number of dendrite branches found in the PFS-F3 treated cells was related to the polymerization and arrangement of F-actin. It can be concluded that the PFS-F3 extract lowered UVB-induced hyperpigmentation through its antioxidant property, which lowered tyrosinase function through the suppression of MITF and was related to F-actin polymerization and arrangement associated with cellular differentiation. Such activities were attributed to the action of the PCT contained in the PFS-F3 extract. Moreover, treatment with PFS-F3 did not affect the viability of the B16F10 cells. The mechanism of PCT on the mitigation of free radical molecules was explained as donating 4'-H atoms to the free radical molecules while the 3'-OH hydrogen atoms bonded strongly to the adjacent PCT molecules. Moreover, the motion of the hydroxyl hydrogen atoms produces a second hydrogen bond chain, which facilitates the transfer of the hydrogen atoms of PCT with low energy (Rossi et al., 2008). However, Medrano-Padial et al. (2021) reported that pure PCT slightly altered the viability of B16 cells even when used at low concentrations. With its reputation as a high-antioxidant food, PFS should be investigated for other effects related to oxidative stress, such as skin aging. Therefore, this proposed investigation will be considered as our future project.

CONCLUSION

The piceatannol-rich extract derived from *Passiflora edulis* fruit seeds demonstrated efficacy in inhibiting morphological differentiation in UVB-induced B16F10 cells, resulting in the reduction of melanin production. This effect was achieved by suppressing MITF mRNA functions and F-actin polymerization, which is attributable to the decrease in cellular oxidant levels. Consequently, the piceatannol-rich extract from *P. edulis* fruit seeds emerges as a promising and safe candidate for anti-hyperpigmentation interventions.

CONFLICT OF INTEREST

The authors declare no conflicts of interest.

ACKNOWLEDGMENTS

The funding of this research was supported by Research and Researchers for Industries (RRI), Thailand Science Research and Innovation (TSRI), with the cooperation of Detox Thailand Co., Ltd. (Grant number PHD61I0034). The authors also thank the Department of Pathobiology, Faculty of Science, Mahidol University, provided the reagents and instruments used in this project.

REFERENCES

Alam MB, Ahmed A, Motin MA, Kim SW, Lee SH (2018) Attenuation of melanogenesis by *Nymphaea nouchali* (Burm. f) flower extract through the regulation of cAMP/CREB/MAPKs/MITF and proteasomal degradation of tyrosinase. Sci Rep 8: 13928. https://doi.org/10.1038/s41598-018-32303-7

Carreira S, Goodall J, Denat L, Rodriguez M, Nuciforo P, Hoek KS, Testori A, Larue L, Goding CR (2006) *Mitf* regulation of *Dia1* controls melanoma proliferation and invasiveness. Genes Dev 20(24): 3426–3439. https://doi.org/10.1101/gad.406406

Chalortham N, Povichit N, Kreawsa S, Moonsawat K, Yasamoot D, Jaisit N, Saefong C, Leepatanakun L, Pongtakam C, Na Lamphun J, Suwannalert P, Ezure Y (2019) Comparison of piceatannol content in seed coat and embryo of passion fruit. Thai Bull Pharm Sci 14(1): 35–48. https://doi.org/10.14456/tbps.2019.4

D'Mello SAN, Finlay GJ, Baguley BC, Askarian-Amiri ME (2016) Signaling pathways in melanogenesis. Int J Mol Sci 17(7): 1144. https://doi.org/10.3390/ijms17071144

D'Orazio J, Jarrett S, Ortiz AA, Scott T (2013) UV radiation and the skin. Int J Mol Sci 14(6): 12222–12248. https://doi.org/10.3390/ijms140612222

Díaz-Camino C, Conde R, Ovsenek N, Villanueva MA (2005) Actin expression is induced and three isoforms are differentially expressed during germination in *Zea mays*. J Exp Bot 56(412): 557–565. https://doi.org/10.1093/jxb/eri034

González-Gutiérrez AG, Verdín J, Rodríguez-Garay B (2020) Simple whole-mount staining protocol of F-actin for studies of the female gametophyte in Agavoideae and other Crassinucellate ovules. Front Plant Sci 11: 384. https://doi.org/10.3389/fpls.2020.00384

Hobanthad T, Maneetong S (2019) Simple extraction for the scanning of antioxidant activity of vegetables and fruits in Buriram, Thailand by DPPH, ABTS and FRAP assays. SNRU J Sci Tech 11(3): 114–121.

Ishimoto T, Mori H (2022) Control of actin polymerization via reactive oxygen species generation using light or radiation. Front Cell Dev Biol 10: 1014008. https://doi.org/10.3389/fcell.2022.1014008

Kamiński K, Kazimierczak U, Kolenda T (2022) Oxidative stress in melanogenesis and melanoma development. Contemp Oncol 26(1): 1–7. https://doi.org/10.5114/wo.2021.112447

Katoh K, Kano Y, Noda Y (2011) Rho-associated kinase-dependent contraction of stress fibres and the organization of focal adhesions. J R Soc Interface 8: 305–311. https://doi.org/10.1098/rsif.2010.0419

Kawakami A, Fisher DE (2017) The master role of microphthalmia-associated transcription factor in melanocyte and melanoma biology. Lab Invest 97(60): 649–656. https://doi.org/10.1038/labinvest.2017.9

Kim HR, Lee SH, Noh EM, Oh BJ, Kim SY, Park MH (2023) Anti-melanogenic effect of Moju through inhibition of tyrosinase activity. Mol Cell Toxicol. https://doi.org/10.1007/s13273-022-00329-8

Knapp SK, Iden S (2020) Melanocyte differentiation and epidermal pigmentation is regulated by polarity proteins. bioRxiv 2020.04.20.051722. https://doi.org/10.1101/2020.04.20.051722

Lawag IL, Nolden ES, Schaper AAM, Lim LY, Locher C (2023) A modified Folin-Ciocalteu assay for the determination of total phenolics content in honey. Appl Sci 13(4): 2135. https://doi.org/10.3390/app13042135

Li M, Knapp SK, Iden S (2020) Mechanisms of melanocyte polarity and differentiation: What can we learn from other neuroectoderm-derived lineages? Curr Opin Cell Biol 67: 99–108. https://doi.org/10.1016/j.ceb.2020.09.001

Matsui Y, Sugiyama K, Kamei M, Takahashi T, Suzuki T, Katagata Y, Ito T (2010) Extract of passion fruit (*Passiflora edulis*) seed containing high amounts of piceatannol inhibits melanogenesis and promotes collagen synthesis, J Agric Food Chem 58(20): 11112–11118. https://doi.org/10.1021/jf102650d

Medrano-Padial C, Prieto AI, Puerto M, Pichardo S (2021) Toxicological evaluation of piceatannol, pterostilbene, and ε-viniferin for their potential use in the food industry: A review. Foods. 10(3): 592. https://doi.org/10.3390/foods10030592

Nguyen NT, Fisher DE (2019) MITF and UV responses in skin: From pigmentation to addiction. Pigment Cell Melanoma Res 32(2): 224–236. https://doi.org/10.1111/pcmr.12726

Pintor AVB, Queiroz LD, Barcelos R, Primo LSG, Maia LC, Alves GG (2020) MTT versus other cell viability assays to evaluate the biocompatibility of root canal filling materials: A systematic review. Int Endod J 53(10): 1348–1373. https://doi.org/10.1111/iej.13353

Ravanat JL, Douki T, Cadet J (2001) Direct and indirect effects of UV radiation on DNA and its components. J Photochem Photobiol B 63(1-3): 88–102. https://doi.org/10.1016/s1011-1344(01)00206-8

Rieger AM, Nelson KL, Konowalchuk JD, Barreda DR (2011) Modified annexin V/propidium iodide apoptosis assay for accurate assessment of cell death. J Vis Exp (50): 2597. https://doi.org/10.3791/2597

Rodboon T, Okada S, Suwannalert P (2020) Germinated riceberry rice enhanced protocatechuic acid and vanillic acid to suppress melanogenesis through cellular oxidant-related tyrosinase activity in B16 cells. Antioxidants. 9(3): 247. https://doi.org/10.3390/antiox9030247

Rossi M, Caruso F, Opazo C, Salciccioli J (2008) Crystal and molecular structure of piceatannol; scavenging features of resveratrol and piceatannol on hydroxyl and peroxyl radicals and docking with transthyretin. J Agric Food Chem 56(22): 10557–10566. https://doi.org/10.1021/jf801923j

Wu QY, Fung AHY, Xu ML, Kaman P, Etta YLL, Xiang PK, Yao P, Xiong QP, Dong TTX, Tsim KWK (2018) Microphthalmia-associated transcription factor up-regulates acetylcholinesterase expression during melanogenesis of murine melanoma cells. J Biol Chem 293(37): 14417–14428. https://doi.org/10.1074/jbc.RA118.003729

Wu QY, Wong ZCF, Wang C, Fung AHY, Womg EOY, Chan GKL, Dong TTX, Chen Y, Tsim KWK (2019) Isoorientin derived from *Gentiana veitchiorum* Hemsl. flowers inhibits melanogenesis by down-regulating MITF-induced tyrosinase expression. Phytomedicine 57: 129–136. https://doi.org/10.1016/j.phymed.2018.12.006

Zolghadri S, Beygi M, Mohammad TF, Alijanianzadeh M, Pillaiyar T, Garcia-Molina P, Garcia-Canovas F, Munoz-Munoz J, Saboury AA (2023) Targeting tyrosinase in hyperpigmentation: Current status, limitations and future promises. Biochem Pharmacol 212: 115574. https://doi.org/10.1016/j.bcp.2023.115574

AUTHOR CONTRIBUTION:

Contribution	Kunsorn P	Payuhakrit W	Povichit N	Suwannalert P
Concepts or ideas	x			x
Design	x			x
Definition of intellectual content	x			x
Literature search	x			
Experimental studies	x	x	x	
Data acquisition	x	x	x	x
Data analysis	x	x		x
Statistical analysis	x			
Manuscript preparation	x		x	
Manuscript editing	x	x		
Manuscript review	x	x	x	x

Citation Format: Kunsorn P, Payuhakrit W, Povichit N, Suwannalert P (2024) Piceatannol-rich extract from *Passiflora edulis* Sims seeds attenuates morphological differentiation through the reduction of MITF mRNA expression and F-actin polymerization in UVB-induced hyperpigmented B16F10 cells. J Pharm Pharmacogn Res 12(5): 900–910. https://doi.org/10.56499/jppres23.1717_12.5.900